Structural Monitoring and Maintenance, *Vol. 11, No. 4 (2024) 297-313*
https://doi.org/10.12989/smm.2024.11.4.297

Cyclic in-plane performance assessment of damaged masonry walls retrofitted by FRP layouts

Nima Moradi[a], Mahdi Yazdani* and Hanan Al Sachit[b]

Department of Civil Engineering, Faculty of Engineering, Arak University, Arak, Iran

(*Received July 19, 2024, Revised November 6, 2024, Accepted November 8, 2024*)

Abstract. There are various retrofitting strategies for strengthening damaged masonry walls. GFRPs are known as one of the new FRP-reinforcing techniques that are widely employed in masonry constructions. The purpose of this study is to evaluate the in-plane performance of damaged masonry walls which are strengthened by different GFRP configurations utilizing macro-scale numerical approach. To achieve this aim, firstly, a macro-scale numerical model of a masonry wall is simulated by finite element method in ABAQUS software and it is validated with an experimental result under a combination of a pre-compressive vertical and a horizontal cyclic loading. Secondly, according to constitutive equation-based methods, damaged areas which were observed in the experimental test are assigned to the validated model and the wall is retrofitted with six different GFRP layouts including Circuit, Vertical, Horizontal, H-shape, I-shape and Plus. Lastly, the in-plane cyclic behavior of walls is conducted and compared in terms of strength, stiffness, energy absorption and efficiency. The results revealed that the Horizontal and H-shape layouts have better performances than the Circuit and I-shape configurations. The Circuit and Horizontal configurations displayed quite similar resistance as well as H-shape and I-shape patterns. It was also observed that the Vertical configuration is the most effective GFRP layout since it provides the most enhanced in-plane resistance (51.91%) and dissipated energy (83.88%) with the highest efficiency index.

Keywords: damaged masonry walls; dissipated energy; finite element simulation; GFRP layouts; in-plane cyclic loading

1. Introduction

Masonry walls are identified as essential structural elements in the ancient buildings and are commonly used in the contemporary constructions due to their durability, strength, and low maintenance as infills and partition walls. Although these elements are seismically vulnerable, they are playing a crucial role in resisting seismic excitations in the old masonry structures during earthquakes. It has been observed that the existing unreinforced masonry walls (URMs) were significantly damaged or even collapsed thoroughly under seismic loads, since they are basically designed to withstand gravity loads (Kabir and Kalali 2012, Kalali and Kabir 2012). It has to be mentioned that due to the insufficient in-plane and out-of-plane resistance of URMs and their low

*Corresponding author, Associate Professor, E-mail: m-yazdani@araku.ac.ir
[a]M.Sc., E-mail: nima.moradi6787@gmail.com
[b]M.Sc., E-mail: h1531989@gmail.com

http://www.techno-press.org/?journal=smm&subpage=7 ISSN: 2288-6605 (Print), 2288-6613 (Online)

ductility, the engineers have developed various techniques for retrofitting masonry walls such as ferrocement, shotcrete, grout injection, external reinforcement, post tensioning and center core (Kalali and Kabir 2012), in which among them, Fibre Reinforced Polymers (FRPs) have become increasingly popular in the last decade. FRP composites are also easy to install and require little maintenance, making them an attractive solution for rehabilitation of masonry walls.

The advent of FRP-reinforced technique for retrofitting masonry walls was found cost-effective and practical by researchers, since it not only leads to remarkable enhancements in both load-carrying capacity and deformation of the wall but also improves its durability, stiffness, corrosion and resistance against cracking. It should be noted that the quantity, type and layout of FRPs have extreme effects on the amount of capacity enrichment of masonry elements (Kabir and Kalali 2012). FRP composites are lightweight, high-strength materials made of fibers such as carbon, glass or aramid embedded in a polymer matrix. In the following paragraphs, previous studies related to masonry walls and FRP-reinforced technique that have been conducted are reported.

Kalali and Kabir conducted an experimental investigation on the in-plane performance of masonry walls retrofitted with Glass Fiber Reinforced Polymers (GFRPs). The specimens were tested under a combination of vertical load and in-plane cyclic load. The research revealed that the GFRP retrofitting technique has a significant effect on the in-plane resistance, deformation capacity and energy absorption of masonry walls (Kalali and Kabir 2012). Kabir and Kalali studied the in-plane cyclic response of unreinforced shear walls made of perforated bricks and FRP-strengthened masonry walls through finite element method. The numerical models were subjected to a pre-compressive vertical load and an in-plane cyclic loading simultaneously. The study included examining the in-plane behavior of walls with openings and different aspect ratios reinforced with various strengthening configurations of FRP (Kabir and Kalali 2012). Zhang *et al.* developed finite element models to examine the seismic behavior of masonry walls retrofitted with Basalt Fiber Reinforced Polymers (BFRPs). The developed finite element models were accurately capable of predicting the shear resistance of masonry walls and also reflecting damage progressive in them before and after BFRP-reinforcement under in-plane cyclic loading. The numerical results of their study were in close agreement with experimental tests in terms of peak strength and stiffness degradation (Zhang *et al*. 2016).

Abdulla *et al.* examined the three-dimensional nonlinear response of masonry walls subjected to monotonic and cyclic loadings using a simplified micro-model approach. They proposed the extended finite element method (XFEM) for simulating and investigating crack propagation in masonry models. The approach was successfully capable of capturing failure modes and nonlinear response of masonry walls (Abdulla *et al.* 2017). Vega and Torres conducted experimental study to obtain the in-plane behavior of masonry walls reinforced with Carbon Fiber Reinforced Polymers (CFRPs) under lateral static and cyclic loadings. The results showed that although unreinforced masonry walls have low resistance and ductility, CFRP-strengthening technique can significantly enhance the ultimate load and deformation capacity of walls (Vega and Castellanos 2018).

Shakarami *et al*. evaluated a parametric study on confined masonry walls using finite element micro-modeling technique. The walls were assembled in different aspect and reinforcement ratios and were subjected to the in-plane cyclic loads using LS-DYNA environment. The force-displacement curves were adopted for validation process of numerical models with experimental tests conducted previously. The results indicated that the in-plane performance of masonry walls in terms of ductility, capacity and energy absorption can be significantly affected by the aspect ratio of the wall (Shakarami *et al*. 2020). Yacila *et al*. studied the in-plane behavior of confined masonry walls both numerically and experimentally. They simulated the walls through macro-modeling

approach in ABAQUS software. The nonlinear behavior of concrete and masonry materials were modeled by concrete damaged plasticity model (CDP). Experimental tests were also carried out to validate numerical models. Capacity curves and cracking patterns of the experimental and numerical models were compared and a good agreement was observed between two approaches (Yacila *et al.* 2019).

Komurcu and Gedikli adopted micro and macro modeling approaches to numerically simulate the structural behavior of a masonry wall. It was revealed that micro and macro approaches have severe contrasts in the material identification and crack propagations of walls (Kömürcü and Gedikli 2019). Borah *et al.* developed a numerical finite element model for simulating the structural response of confined masonry walls subjected to in-plane seismic actions. They designed and constructed a masonry wall specimen based on Mexican practice and then they tested the wall under in-plane loadings. Borah *et al.* used ABAQUS software for simulating walls and adopted CDP model for considering material's nonlinear behavior. The proposed numerical model displayed close agreement with experimental results (Borah *et al.* 2020). Howlader *et al.* carried out experimental study on unreinforced masonry walls subjected to cyclic loading. Among the findings of their research, it was showed that the geometry of the wall and the amount of pre-compression loading can have significant effects on the failure mode and the capacity of wall. It was also revealed that the ASCE guidelines are in good agreement with test results in terms of wall strength, in-plane stiffness and failure mode (Howlader *et al.* 2020).

A database of 120 FRP-retrofitted wall samples was created by Hadzima-Nyarko et. al based on the previous studies and different strategies for computing load-carrying capacity of FRP-retrofitted walls were detailed and discussed. Hadzima-Nyarko *et al.* also compared the results of experimental researches with findings obtained from formulas presented in building codes and literature (Hadzima-Nyarko *et al.* 2021). Ma *et al.* investigated how in-plane failure mechanism of URMs can be affected by different factors such as aspect ratio of pier, stiffness ratio of pier to spandrel and vertical load (Ma *et al.* 2022). Different reinforcing methods including Fibre Reinforced Polymers (FRPs), Textile-reinforced Mortars (TRMs) and Engineered Cementitious Composites (ECCs) were employed to strengthen the unreinforced masonry wall by Deng *et al.*. It was showed that the TRM-reinforcing technique causes the specimens to exhibit the maximum midspan deformation and ECCs also indicated the most bearing strength and ductility (Deng *et al.* 2023). Sleiman *et al.* studied the in-plane lateral response of UHPC-strengthened infilled RC frames under cyclic loading through an experimental program. Results indicated that UHPC-strengthening method can enhance the peak lateral resistance of specimens 2 and 1.3 times of as-built and FRP-strengthened specimens, respectively. It was also found that the UHPC-retrofitting technique can lead to a significant increase in initial stiffness and energy dissipation of specimens (Sleiman *et al.* 2024).

The performance of two strengthening strategies including non-prestressed and prestressed near surface mounted GFRP bars was investigated and compared with unreinforced masonry walls in terms of ultimate strength, failure displacement and ductility by Kashani *et al.* (2023). The in-plane response of historical masonry walls with various brickwork arrangements was conducted numerically by Moradi et al. using ABAQUS finite element software. The numerical models were implemented through simplified micro-scale modeling approach and the CDP nonlinear model was used to simulate the nonlinear behavior of masonry units. Moradi *et al.* also evaluated the seismic performance of the masonry walls based on the Iranian seismic code (Moradi *et al.* 2024). Yazdani and Zirakbash examined the in-plane cyclic performance of masonry arch bridges which were retrofitted with sprayed concrete technique. The hysteresis and enveloping capacity curves of both

the retrofitted and non-retrofitted bridge were carried out through finite element method and compared in terms of energy absorption and degradation of material (Yazdani and Zirakbash 2024).

This study focuses on developing an efficient macro-scale numerical modeling for simulating the precise behavior of damaged masonry walls retrofitted by GFRP layouts under cyclic loading. To this aim, the study has been divided into four phases. In the first phase, the numerical simulation of a masonry wall is implemented in ABAQUS software using macro-scale modeling.

The wall is applied to a combined in-plane vertical compressive and lateral cyclic load. After validation process of numerical model with experimental results using hysteresis curves and failure modes, in the second phase, a new validated macro model of the masonry wall with simulated damaged elements is implemented and then subjected to the same loading procedure. In the third phase, the simulated damaged wall is retrofitted with GFRPs of six different layouts including Circuit, Vertical, Horizontal, H-shape, I-shape and Plus and applied to the in-plane vertical and cyclic lateral loads simultaneously. Finally in the fourth phase, a comparison between the in-plane performance of the retrofitted and non-retrofitted masonry walls and different GFRP patterns in terms of wall's strength, in-plane stiffness, energy absorption and efficiency are presented and discussed thoroughly.

2. Validation of numerical model

Since masonry consists of two distinct elements including units and mortar, it has an inhomogeneous texture, therefore simulating the complex behavior of this common material has always been a challenging issue (Kömürcü and Gedikli 2019). Although, the experimental approach is recognized as the best method for conducting masonry behavior accurately in terms of load-carrying capacity, deformation, failure mode and so on, it is almost identified as the most expensive and time-consuming approach. Additionally, it has to be noted that the experimental frameworks need precise calibration control of laboratory equipment, otherwise it would cause unavoidable errors in detection and monitoring the results. Hence, in recent decades numerical modeling techniques have been developed as an appropriate alternative to the experimental research, since they are applicable to complicated configurations and can provide an accurate simulation of reality. In term of masonry simulation the numerical methods can be classified into different approaches including finite (Agnihotri *et al.* 2013, Aref and Dolatshahi 2013, Burnett *et al.* 2007, Milani 2008) and discrete element methods (Lemos 2007, Sarhosis and Sheng 2014). Finite element method which is identified as the most desired and widely-spread technique of the numerical modeling approaches among the researchers is categorized in three different methods including micro-scale, meso-scale and macro-scale models (Aref and Dolatshahi 2013).

However, the micro-scale modeling technique is considered as the most precise method for simulating the behavior of a masonry structure, it carries high computational efforts and extreme time-consumption, since mortar joints, masonry units and their interfaces are individually simulated. Unlike the micro-scale modeling method in which the linear and non-linear mechanical behavior of materials can separately be defined and assigned to the related elements, in macro-scale technique, a continuum homogenous model is considered and an equivalent material property is defined for the whole geometry which can significantly reduce the computational cost. Meso-scale modeling approach is quite similar to micro-scale modeling method and its main difference is that the mortar joints are not individually modeled in masonry; instead, the effect of mortar layers is considered as interfaces between masonry units. This method has also been found

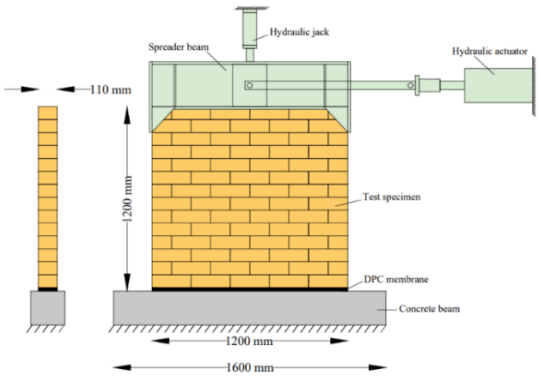

Fig. 1 Test set-up based on the Ref (Mojsilović *et al*. 2010)

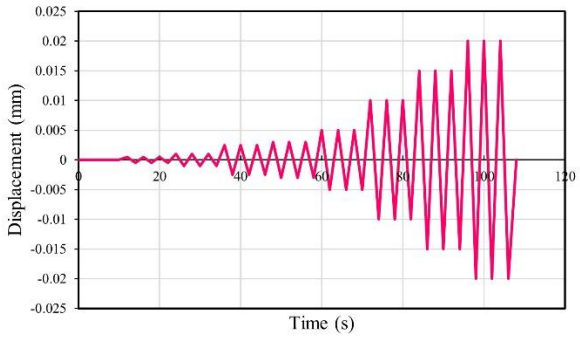

Fig. 2 Applied in-plane displacement-time history in experimental test (Mojsilović *et al*. 2010)

to be effective for modeling large elements of masonry structures (Zhang *et al.* 2016).

In this study, it was decided to develop a macro-scale model for simulating the in-plane behavior of damaged masonry walls retrofitted with GFRP layers under cyclic loading through ABAQUS finite element software. To this aim, a laboratory test which was carried out by Mojsilovic et. al, was adopted to validate the numerical model (Mojsilović *et al.* 2010). In the mentioned study, a masonry wall of dimensions $1.2\,m \times 1.2\,m \times 0.11\,m$ which was labelled as B3-2 in the experimental study, was built using extruded clay bricks. The wall was assembled on a RC beam of dimensions $1.6\,m \times 0.2\,m \times 0.2\,m$ and a damp-proof course (DPC) was placed between the bottom of the wall and the RC beam and afterward the wall was cured in the air for 28 days. The numerical macro-scale model of the masonry wall was implemented in ABAQUS software (Abaqus & RI) according to Fig. 1. The wall was initially subjected to a pre-compressive vertical stress of 0.7 MPa and then applied to a cyclic shear loading by means of a hydraulic actuator according to Fig. 2.

In the numerical macro-scale modeling, surface-based cohesive element was adopted to simulate the damp-proof course's (DPC) behavior between the wall and the reinforcement beam.

This method is considered to define the contact behavior between two surfaces which is governed by Eq. (1).

Table 1 Mechanical properties of the contact interface

Stiffness coefficients (kN/m^3)			Damage initiation (kN/m^2)			Damage evolution (J)
K_{nn}	K_{ss}	K_{tt}	t_n (Mode I)	t_s (Mode II)	t_t (Mode III)	G_f
63E6	25E6	25E6	40	28	28	1

Table 2 Concrete damaged plasticity of masonry wall

ψ	ϵ	σ_{b0}/σ_{c0}	K_c	Viscosity
30	0.1	1.16	0.667	0.0001

$$t = \begin{Bmatrix} t_n \\ t_s \\ t_t \end{Bmatrix} = \begin{bmatrix} K_{nn} & K_{ns} & K_{nt} \\ K_{ns} & K_{ss} & K_{st} \\ K_{nt} & K_{st} & K_{tt} \end{bmatrix} \begin{Bmatrix} \delta_n \\ \delta_s \\ \delta_t \end{Bmatrix} = K\delta \quad (1)$$

K, t and δ represent the stiffness, shear stress and separation vectors. The indexes $n, s\ and\ t$ are corresponded with normal and two transverse directions, respectively. The linear traction-separation parameters were derived during the model updating process and are reported in Table 1. The damage evolution of surface-based cohesive behavior was defined with fracture energy which is equal to the area under the traction-separation curve. The tangential behavior of the wall-RC beam interface was assumed as 0.38 for the friction coefficient. Moreover, the hard contact was considered for normal behavior of the interface which is defined by using contact pressure-overclosure relationship (Doran *et al*.).

The mechanical behavior of masonry wall in terms of density and Poisson's ratio were assumed as $2000\,kg/m^3$ and 0.15. Based on Ref (Kaushik *et al*. 2007), the compressive (f_m) and tensile strength (f_t) of masonry wall were calculated using Eqs. (2) and (3).

$$f_m = 0.63 f_{\mathrm{br}}^{0.49} f_{mr}^{0.32} \quad (2)$$

$$f_t = 0.1 f_m \quad (3)$$

f_{br} and f_{mr} are the compressive strength of clay brick and mortar respectively. The modulus of elasticity of masonry wall (E_m) was considered as 550 times the compressive strength of f_m. Also, the strain corresponded to the compressive strength of masonry wall (ε_m) was obtained using Eq. (4). The (c_j) coefficient used in Eq. (4) is also calculated by Eq. (5).

$$\varepsilon_m = c_j \frac{f_m}{E_m^{0.7}} \quad (4)$$

$$c_j = \frac{0.27}{f_{mr}^{0.25}} \quad (5)$$

The stress-strain curves for compressive and tensile behavior of masonry wall were finally derived according to Fig. 3 and defined through CDP model in ABAQUS software. The constitutive parameters used in CDP model in terms of dilation angle (ψ), eccentricity (ϵ), initial biaxial compressive yield stress to initial uniaxial compressive yield stress $(\sigma_{b0}/\sigma_{c0})$, shape of yield stress (K_c) and viscosity were assumed based on Table 2. The value of K_c which is the ratio between the second stress invariant on the tensile meridian, is always taken between 0 and 1.

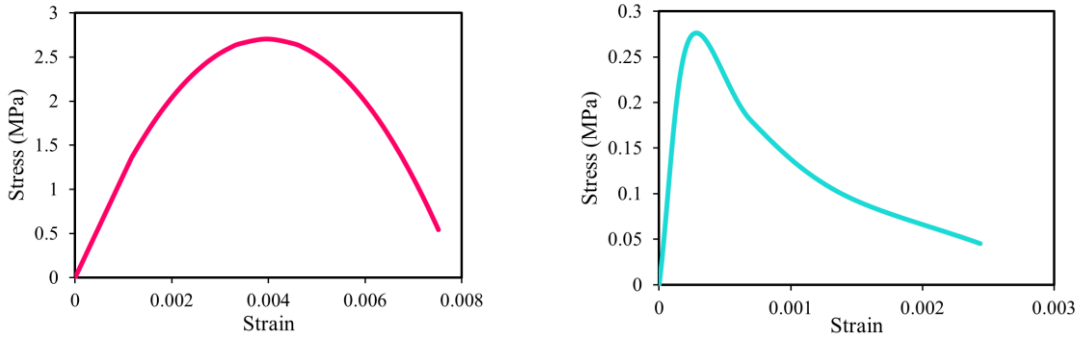

(a) (b)

Fig. 3 The stress – strain curves of masonry wall in (a) compression and (b) tension

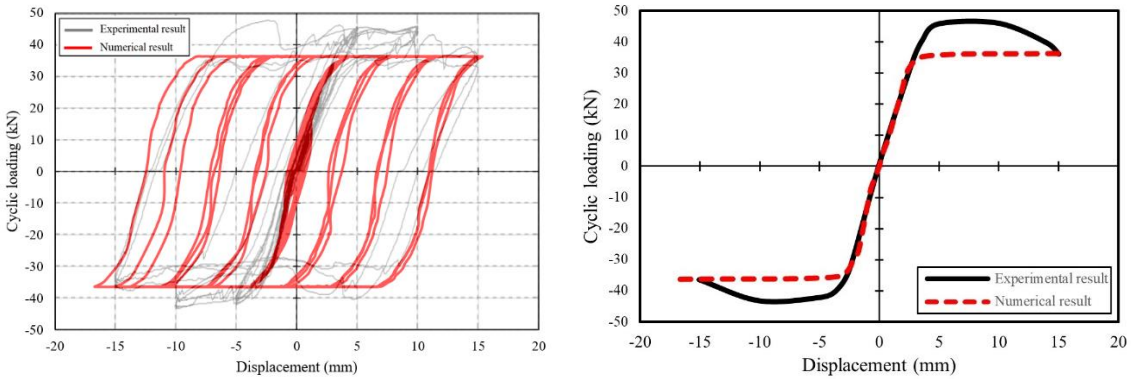

(a) (b)

Fig. 4 Comparison of numerical and experimental (a) hysteresis curves and (b) envelope curves

The dilation angle shows the possible changes in material's volume influenced by compound stress. This parameter is considered to be between $10°$ and $36°$ for URM walls (Abasi *et al.* 2020, D'Altri *et al.* 2018, Deng and Yang 2020, Doran *et al.* 2022, Naciri *et al.* 2020). Viscosity parameter should be assumed in the model, since it helps solving convergence problems when the material's stiffness and strength tend to decrease (Doran *et al.* 2022).

The wall was restrained in out-of-plane transitional direction and the concrete footing beam was fixed in both transitional and rotational degrees of freedom. Since the pre-compressive vertical load was distributed through a steel beam in the experimental test, the load was defined as a pressure vertical stress which was applied to the top surface of the wall. The in-plane cyclic shear load was also applied to a reference point which had been coupled to the wall's top surface.

The numerical model of wall was meshed with 8-node linear cubic elements (C3D8R) and a $0.12\ m \times 0.12\ m \times 0.11\ m$ element size was considered for the wall. The numerical analysis was conducted in 1265 steps using implicit integration method. The minimum and maximum increment size was assumed as 1E-15 and 1, respectively.

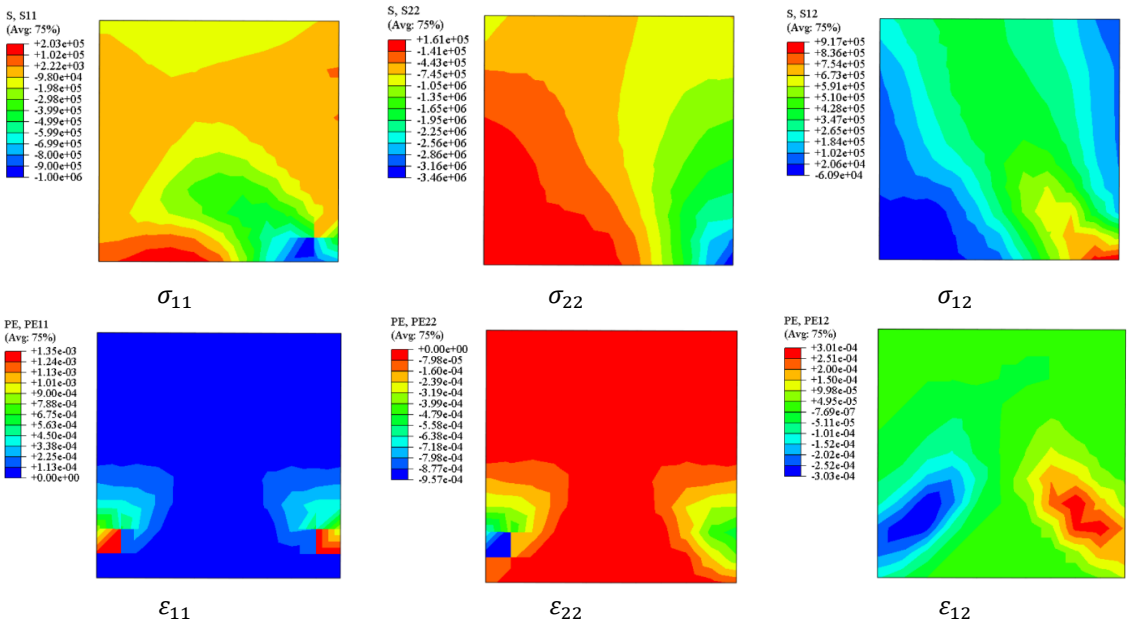

(a)

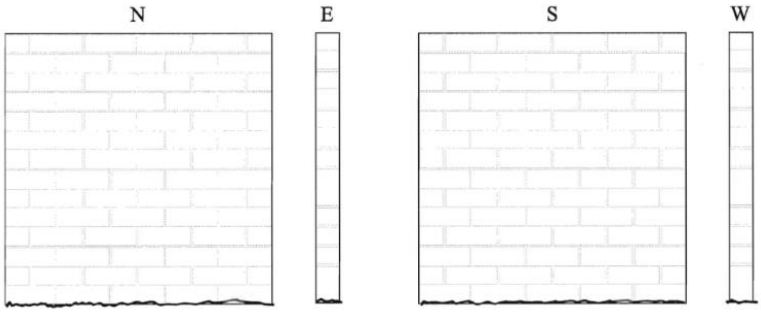

(b)

Fig. 5 Failure mode of considered masonry wall (a) numerical results and (b) experimental result (Mojsilović *et al.* 2010)

Table 3 Discrepancy between experimental and numerical models

	Maximum Displacement (mm)		Maximum Strength (kN)	
	Push	Pull	Push	Pull
Experimental	15	-15.06	46.08	-43.21
Numerical	14.98	-16.66	36.29	-36.29
Error	0.13%	9.6%	21.24%	16.01%

The cyclic loading-displacement curve of the proposed numerical model was obtained and compared with the experimental result as displayed in Fig. 4. The numerical result shows a good agreement with experimental study in terms of lateral displacement, strength and initial stiffness

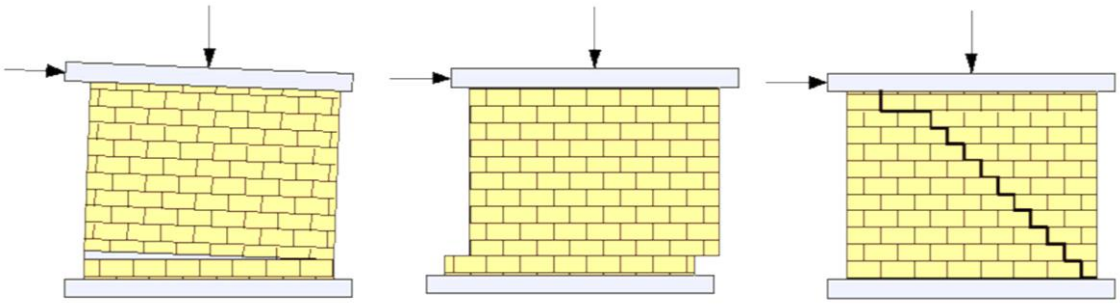

(a) (b) (c)

Fig. 6 Common in-plane failure mode of masonry walls under seismic action. (a) rocking, (b) sliding shear and (c) diagonal shear (Oyguc and Oyguc 2017)

(Table 3). The numerical result of the masonry wall is displayed in Fig. 5(a). Based on the stress and strain contours, it is observed that the wall has failed in sliding shear mode as shown in the experimental result (Fig. 5(b)).

3. Damaged masonry wall modeling

In computational damage mechanics, two means are commonly adopted to simulate damages: 1) geometrical modeling and 2) non-geometrical modeling. In the first technique, the geometry of damages is modeled (Panian and Yazdani 2020), while the second technique considers the effects of damages physically (Yazdani 2021). The non-geometrical technique is further divided into two sub-approaches. The first sub-approach includes constitutive equation-based methods. It does not model damages but treats the area around the cracks as a weak region that can be incorporated in the form of reduced strength or reduced stiffness. The smeared cracking method is among the most widely used techniques of the first non-geometrical procedure. The second non-geometrical sub-approach includes kinematic methods that utilize enrichment methods. Thus, the second non-geometrical sub-approach benefits from the advantages of geometric crack modeling. The extended finite element method is widely used as the second non-geometrical technique (Yazdani and Habibi 2023).

Previous earthquakes have indicated that the failure modes of masonry walls are based on the Fig. 6 (Hadzima-Nyarko *et al*. 2021, Oyguc and Oyguc 2017). So, in this study based on failure mode identification and aspect ratio of considered wall, it was decided to simulate the damaged masonry walls by the first non-geometrical sub-approach technique in the form of reduced strength and stiffness (Mohammadi 2012). To this aim, an almost new linear and non-linear mechanical behavior was defined and assigned to some particular elements of validated numerical model of the masonry wall, as highlighted in Fig. 7(a). The new mechanical behavior of damaged wall in terms of the modulus of elasticity was employed as 0.01 times E_m of the undamaged wall; therefore, the non-linear CDP model parameters were calculated again for the damaged wall (Figs. 7(b)-7(c)). The other parameters such as Poisson's ratio (ν), density (γ), dilation angle (ψ), eccentricity (ϵ), initial biaxial compressive yield stress to initial uniaxial compressive yield stress $(\sigma_{b0}/\sigma_{c0})$, shape of yield stress (K_c) and viscosity were assumed similar to the validated model.

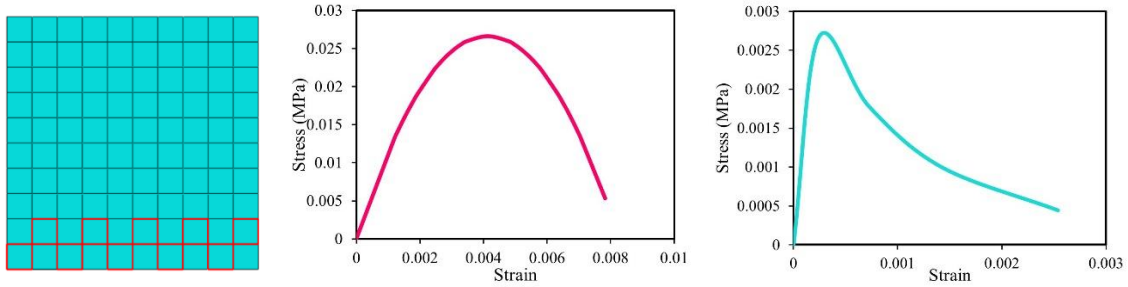

(a) (b) (c)

Fig. 7 Simulation of damaged masonry wall (a) damaged zones, (b) the stress – strain curves in compression and (c) the stress – strain curves in tension

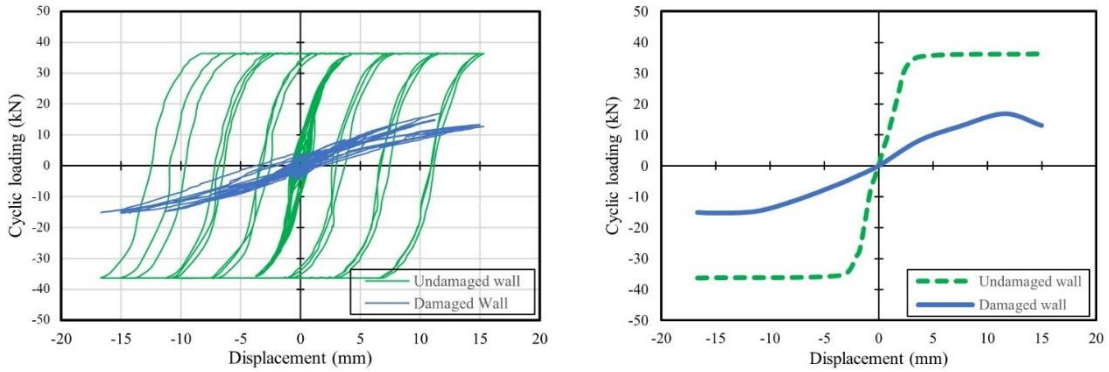

(a) (b)

Fig. 8 Comparison of (a) numerical hysteresis curves and (b) envelope curves of undamaged and damaged walls

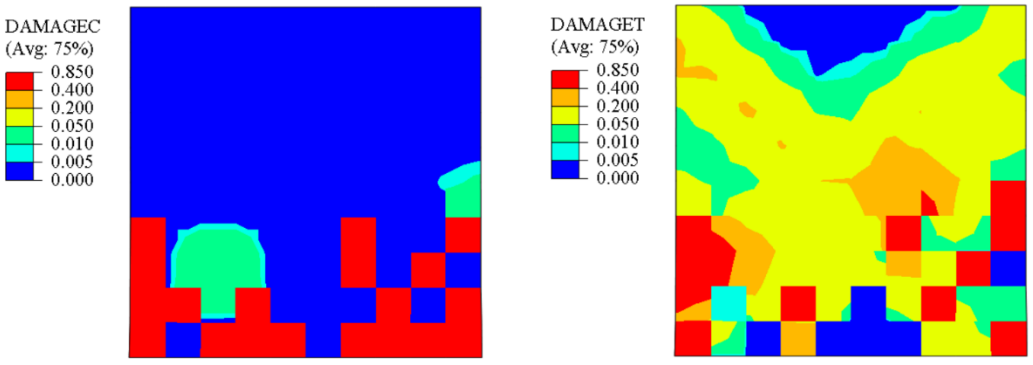

(a) (b)

Fig. 9 The damage index contours of masonry wall for (a) compression and (b) tension

Table 4 Comparing damaged and undamaged wall results

	Initial stiffness (kN/mm)	Maximum Strength (kN)		Energy absorption (kN.m)	
		Push	Pull	Push	Pull
Undamaged wall	13.49	36.29	-36.29	0.484	0.548
Damaged wall	2.20	16.83	-15.32	0.166	0.174
Discrepancy	83.69%	53.62%	57.78%	65.7%	68.25%

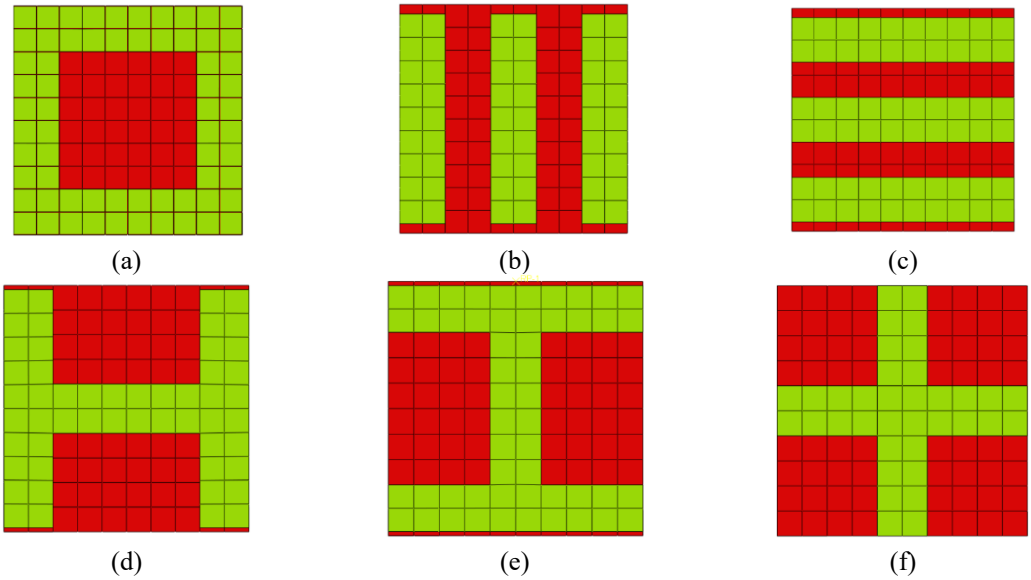

Fig. 10 Different GFRP configurations (a) Circuit, (b) Vertical, (c) Horizontal, (d) H-shape, (e) I-shape and (f) Plus

The in-plane response of the damaged wall was conducted under previous cyclic loading procedure and is reported in Fig. 8. The visualized numerical result of the damaged masonry wall has been also displayed in Fig. 9 based on the damage index. The result shows that the in-plane capacity, initial stiffness and energy absorption of the wall has been significantly decreased after applying damages to the wall. As it is shown in Table 4, the initial stiffness, maximum strength and energy absorption of the damaged wall in comparison with undamaged wall have been reduced by 83.69%, 53.62% and 65.7% in push curves, respectively.

4. GFRP-retrofitted walls modeling

After accruing the natural disaster like earthquake, the damaged structures are retrofitted by efficient and rapid methods to increase the sustainability of cities and societies. Using FRP layouts is one of the most reliable and express method of rehabilitation. Therefore, in this section, six different types of GFRP configurations were adopted to retrofit the damaged masonry wall according to Fig. 10. The mechanical property of the GFRP material was defined based on Table 5.

Table 5 Mechanical behavior of GFRP (Yazdani 2016)

E_1	E_2	E_3	ν_{12}	ν_{13}	ν_{23}	G_{12}	G_{12}	G_{12}
21E9	7E9	7E9	0.26	0.26	0.3	1.52E9	1.52E9	2.65E9

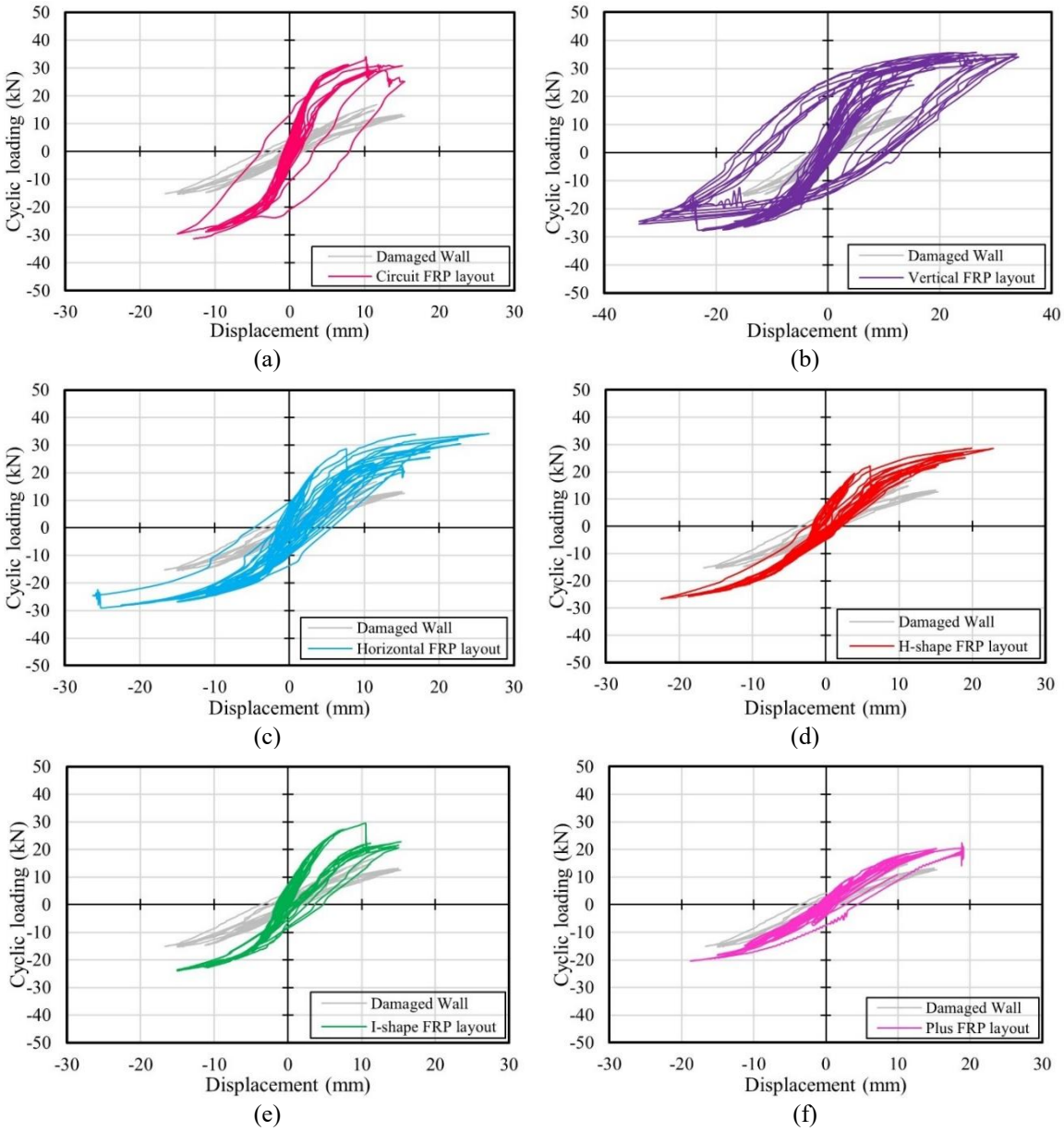

Fig. 11 Hysteresis curves of masonry walls retrofitted by different GFRP layouts (a) Circuit, (b) Vertical, (c) Horizontal, (d) H-shape, (e) I-shape and (f) Plus patterns

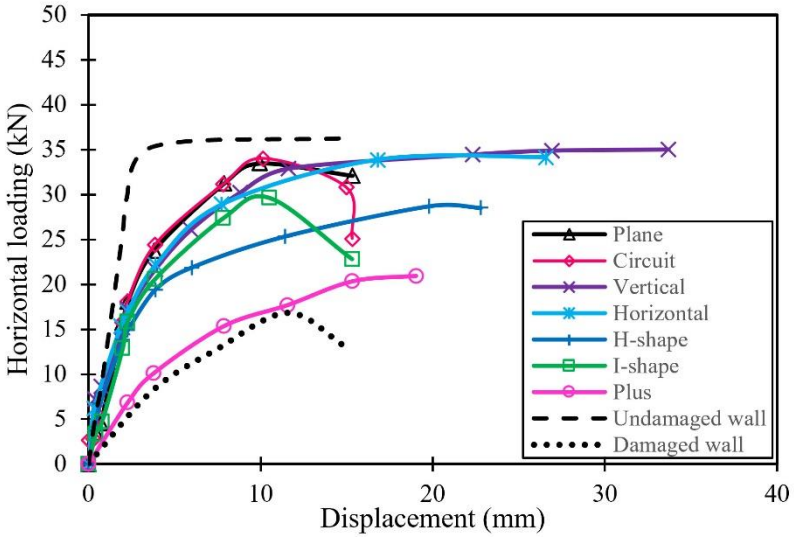

Fig. 12 Skeleton curves of masonry walls retrofitted with different GFRP layouts

Table 6 Comparing skeleton curves results of retrofitted-walls of different GFRP configurations

GFRP layouts	GFRP coverage percent	GFRP area (m^2)	Initial stiffness (kN/mm)	Maximum strength (kN)	Energy absorption (kN.m)	Efficiency index
Circuit	64%	0.9216	9.40	34.01	0.40747	0.340
Vertical	55%	0.792	19.17	35	1.02983	1
Horizontal	60%	0.864	18.30	34.15	0.77056	0.686
H-shape	51%	0.7296	11.03	28.72	0.53132	0.560
I-shape	49%	0.7008	8.15	29.62	0.34328	0.377
Plus	36%	0.5184	3.01	20.94	0.28138	0.418

The GFRP stripes were simulated using shell element and the thickness of stripes was considered as 1.3 mm. The stripes were tied to one side surface of the wall.

4-node linear quad elements (S4R) were utilized for meshing shell models. The implemented numerical models were subjected to a combined vertical and horizontal cyclic loading and their behaviors were conducted as displayed in Fig. 11. Afterward, the skeleton curves of retrofitted masonry walls of different layouts were derived according to Fig. 12 and their performance was compared in terms of initial stiffness, maximum strength, energy dissipation and normalized energy dissipation per area of FRP layouts as efficiency index. (Table 6).

It is apparent from Table 6 that the Vertical GFRP layout displayed the most enhanced resistance and energy absorption, whereas the Plus layout exhibited the least. The Circuit and Horizontal configurations showed almost similar resistance as well as H-shape and I-shape patterns. Additionally, it can be seen that the energy dissipation of the Horizontal, H-shape, I-shape and circuit patterns was achieved between the Vertical and Plus values. Table 6 also displays that the Vertical and Horizontal models revealed the highest initial stiffnesses among the other configurations.

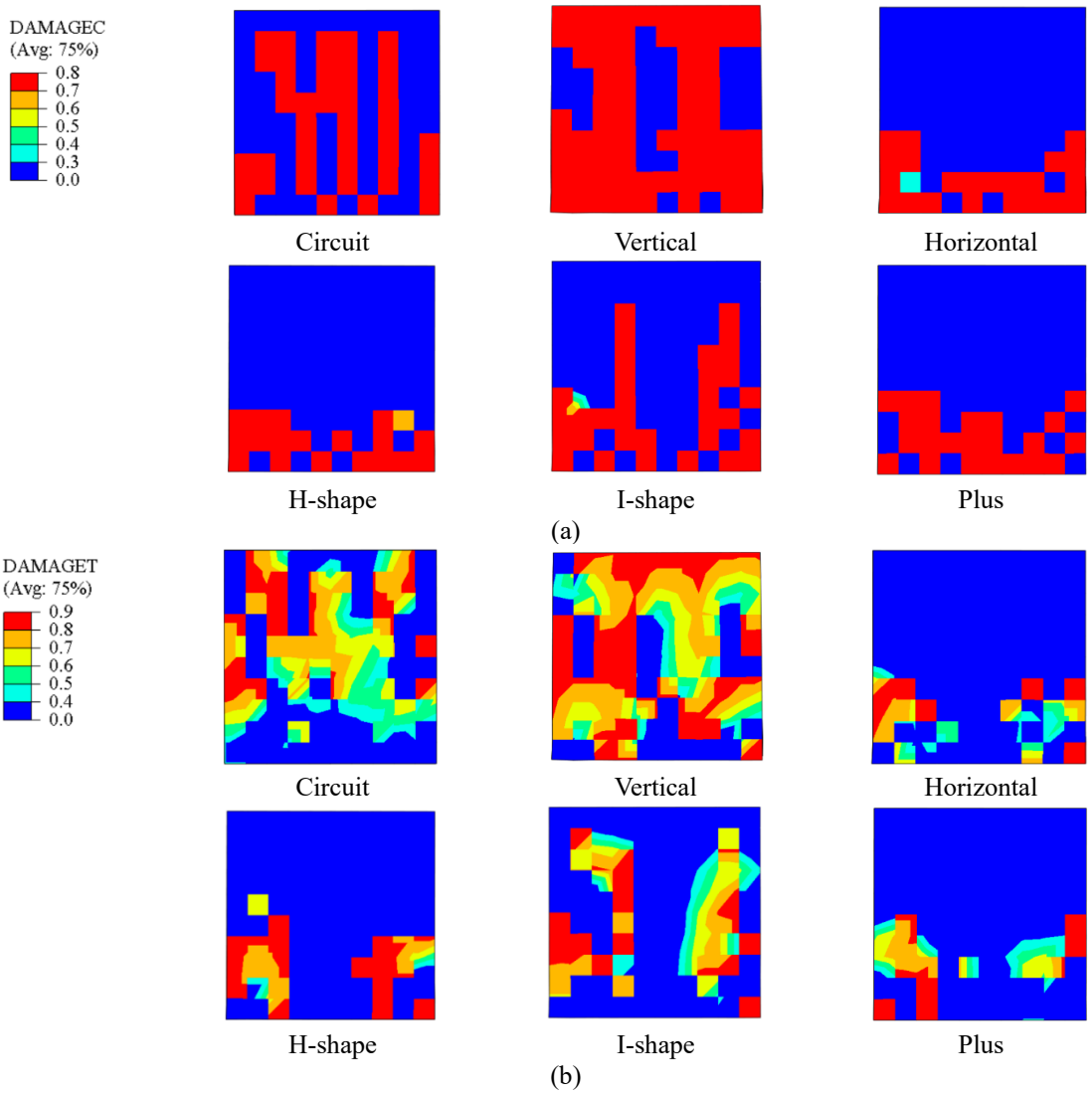

Fig. 13 The damage index contours of different retrofitted masonry wall for (a) compression and (b) tension state

The efficiency index is defined as the ratio between the energy absorption obtained by the wall and the area of GFRP layout which is then normalized by the maximum value of them. The calculated efficiency index is reported in Table 6. It can be realized that the Vertical GFRP layout has the most efficient performance among the other models by the value of one. The Horizontal and H-shape obtained 0.686 and 0.560 values in efficiency, respectively and the Circuit and I-shape showed almost similar performances. Moreover, the Plus layout was recognized as more efficient pattern for retrofitting damaged walls than Circuit and I-shape configurations. The failure mode of GFRP-retrofitted walls is demonstrated in Fig. 13 through damage-C and damage-T contours. It is apparent that the strengthened walls have been mostly damaged in their non-retrofitted areas.

5. Conclusions

Masonry walls are recognized as indispensable structural components in the historical masonry buildings and are also being employed as infill walls and non-structural elements in today's modern buildings. In the previous earthquakes, it was observed that the masonry walls have been damaged and cracked due to their low shear and tensile resistance. Different retrofitting techniques have been discovered to enhance the strength and stability of the damaged masonry constructions such as GFRPs. In this study, a macro-scale numerical model of a masonry wall has been implemented in ABAQUS software and subjected to a combined pre-compressive vertical load and a horizontal cyclic shear loading. After validation process of the numerical macro-scale model with an experimental test, the bottom of the wall which had been significantly affected by the compressive and tensile forces was identified as the damaged area. Afterward, a new masonry wall similar to the validated numerical model was implemented and the damaged elements were simulated in the model through defining a new weaker material property. The proposed model was examined under the in-plane vertical and horizontal loading procedure and the effect of considering damaged elements in the wall was observed. In the next step six different GFRP layouts including Circuit, Vertical, Horizontal, H-shape, I-shape and Plus were adopted for retrofitting the damaged wall. The numerical retrofitted models were evaluated under cyclic shear loading and the hysteresis curves were obtained. The results of the study indicated that:

- The Vertical GFRP layout revealed the most enhanced resistance (51.91%) and dissipated energy (83.88%), whereas the Plus layout exhibited the least.
- The Circuit and Horizontal configurations displayed quite similar strength. The maximum strengths obtained by H-shape and I-shape patterns were also close to each other.
- The Vertical and Horizontal models revealed the highest initial stiffnesses and lateral displacements among the other configurations.
- The in-plane capacity and energy absorption of the wall is significantly affected by the GFRP layout.
- The Vertical configuration was identified as the best GFRP layout for retrofitting the damaged masonry wall since it showed the highest efficiency index among the other retrofitted damaged walls. The Circuit layout was also recognized as the least efficient method for retrofitting damaged masonry walls.

References

Abaqus. (2022), Abaqus, Standard User's Manual Dassault Systèmes Simulia Corporation: Providence. USA: RI.

Abasi, A., Hassanli, R., Vincent, T. and Manalo, A. (2020), "Influence of prism geometry on the compressive strength of concrete masonry", *Constr. Build. Mater.*, **264**, 120182. https://doi.org/10.1016/j.conbuildmat.2020.120182.

Abdulla, K., Cunningham, L. and Gillie, M. (2017), "Simulating masonry wall behaviour using a simplified micro-model approach", *Eng. Struct.*, **151**, 349-365. https://doi.org/10.1016/j.engstruct.2017.08.021.

Agnihotri, P., Singhal, V. and Rai, D. (2013), "Effect of in-plane damage on out-of-plane strength of unreinforced masonry walls", *Eng. Struct.*, **57**, 1-11. https://doi.org/10.1016/j.engstruct.2013.09.004.

Aref, A. and Dolatshahi, K. (2013), "A three-dimensional cyclic meso-scale numerical procedure for simulation of unreinforced masonry structures", *Comput. Struct.*, **120**, 9-23. https://doi.org/10.1016/j.compstruc.2013.01.012.

Borah, B., Kaushik, H. and Singhal, V. (2020), "Finite element modelling of confined masonry wall under in-plane cyclic load", *IOP Conference Series: Materials Science and Engineering*., **936**, 936-931. https://doi.org/10.1088/1757-899X/936/1/012020.

Burnett, S., Gilbert, M., Molyneaux, T., Beattie, G. and Hobbs, B. (2007), "The performance of unreinforced masonry walls subjected to low-velocity impacts: Finite element analysis", *Int. J. Impact Eng.*, **34**, 1433-1450. https://doi.org/10.1016/j.ijimpeng.2006.08.004.

D'Altri, A., Miranda, S., Castellazzi, G. and Sarhosis, V. (2018), "A 3D detailed micro-model for the in-plane and out-of-plane numerical analysis of masonry panels", *Comput. Struct.*, **206**, 18-30. https://doi.org/10.1016/j.compstruc.2018.06.007.

Deng, M., Dong, Z., Dai, J. and Zhao, X. (2023), "Out-of-plane strengthening of URM walls using different fiber-reinforced materials", *Constr. Build. Mater.*, **362**, 129597. https://doi.org/10.1016/j.conbuildmat.2022.129597.

Deng, M. and Yang, S. (2020), "Experimental and numerical evaluation of confined masonry walls retrofitted with engineered cementitious composites", *Eng. Struct.*, **207**, 110249. https://doi.org/10.1016/j.engstruct.2020.110249.

Doran, B., Karslıoğlu, M., Aslan, Z. and Vatansever, C. (2022), "Experimental and numerical investigation of unreinforced masonry walls with and without opening", *Int. J. Architect. Heritage*, **17**, 1-22. https://doi.org/10.1080/15583058.2022.2080611.

Hadzima-Nyarko, M., Čolak, S., Bulajić, B. and Ademovic, N. (2021), "Assessment of selected models for FRP-retrofitted URM walls under in-plane loads", *Buildings*, **11**, 559. https://doi.org/10.3390/buildings11110559.

Howlader, M., Masia, M. and Griffith, M. (2020), "In-plane response of perforated unreinforced masonry walls under cyclic loading: Experimental study", *J. Struct. Eng.*, **146**(6). https://doi.org/10.1061/(ASCE)ST.1943-541X.0002657.

Kabir, M.Z. and Kalali, A. (2012), "In-plane numerical modelling of sterngthened perforated masonry walls using FRP under cyclic loading", *Asian J. Civil Eng.*, **14**(1), 161-179. https://www.magiran.com/paper/1079834.

Kalali, A. and Kabir, M.Z. (2012), "Cyclic behavior of perforated masonry walls strengthened with glass fiber reinforced polymers", *Scientia Iranica*, **19**, 151-165. https://doi.org/10.1016/j.scient.2012.02.011.

kashani, H., Shakiba, M., Bazli, M., Hosseini, S.M., Mortazavi, S.M.R. and Arashpour, A.P.M. (2023), "The structural response of masonry walls strengthened using prestressed near surface mounted GFRP bars under cyclic loading", *Mater. Struct.*, **56**(112). https://doi.org/10.1617/s11527-023-02201-0.

Kaushik, H., Rai, D., Jain, S. and Asce, M. (2007), "Stress-strain characteristics of clay brick masonry under uniaxial compression", *J. Mater. Civil Eng.*, **19**(9). https://doi.org/10.1061/(ASCE)0899-1561(2007)19:9(728).

Kömürcü, S. and Gedikli, A. (2019), Macro and Micro Modeling of the Unreinforced Masonry Shear Walls. **3**, 116-123.

Lemos, J. (2007), "Discrete element modeling of masonry structures", *Int. J. Architect. Heritage*, **1**, 190-213. https://doi.org/10.1080/15583050601176868.

Ma, P., Yao, J. and Hu, Y. (2022), "Numerical analysis of different influencing factors on the in-plane failure mode of unreinforced masonry (URM) structures", *Buildings*, **12**, 183. https://doi.org/10.3390/buildings12020183.

Milani, G. (2008), "3D upper bond limit analysis of multi-leaf masonry walls", *Int. J. Mech. Sci.*, **50**, 817-836. https://doi.org/10.1016/j.ijmecsci.2007.11.003.

Mohammadi, S. (2012), *XFEM Fracture Analysis of Composites*. https://doi.org/10.1002/9781118443378

Mojsilović, N., Simundic, G. and Page, A. (2010), "Masonry wallettes with damp-proof course membrane subjected to cyclic shear: An experimental study", *Constr. Build. Mater.*, **24**, 2135-2144. https://doi.org/10.1016/j.conbuildmat.2010.04.046.

Moradi, N., Yazdani, M., Janbozorgi, F. and Hashemi, S. (2024), "In-plane seismic performance of historical masonry walls with various brick bond patterns using micro-modeling approach", *Asian J. Civil Eng.*, **25**, 1-14. https://doi.org/10.1007/s42107-024-01085-x.

Naciri, K., Issam, A., Chaaba, A. and Al-Mukhtar, M. (2020), "Detailed micromodeling and multiscale modeling of masonry under confined shear and compressive loading", *Practice Periodical on Structural Design and Construction*, **26**(1). https://doi.org/10.1061/(ASCE)SC.1943-5576.0000538.

Oyguc, R. and Oyguc, E. (2017), "2011 Van Earthquakes: Lessons from damaged masonry structures", *J. Perform. Constr. Fac.*, **31**(5), 04017062. https://doi.org/10.1061/(ASCE)CF.1943-5509.0001057.

Panian, R. and Yazdani, M. (2020), "Estimation of the service load capacity of plain concrete arch bridges using a novel approach: Stress intensity factor", *Structures*, **27**, 1521-1534. https://doi.org/10.1016/j.istruc.2020.07.055.

Sarhosis, V. and Sheng, Y. (2014), "Identification of material parameters for low bond strength masonry", *Eng. Struct.*, **60**, 100-110. https://doi.org/10.1016/j.engstruct.2013.12.013.

Shakarami, B., Kabir, M.Z. and Sistani Nejad, R. (2020), "Numerical modeling of a new reinforced masonry system subjected to in-plane cyclic loading", *Scientia Iranica*, **27**(6), 2790-2807. https://doi.org/10.24200/sci.2019.5376.1237.

Sleiman, E., Ferrier, E., Michel, L. and Saidi, M. (2024), "Seismic behavior of masonry-infilled reinforced concrete frames strengthened using ultra-high performance concrete diagonal strips", *Structures*, **59**, 105790. https://doi.org/10.1016/j.istruc.2023.105790.

Vega, C. and Castellanos, N. (2018), "External strengthening of unreinforced masonry walls with polymers reinforced with carbon fiber", *Ingeniería e Investigación*, **38**, 15-23. https://doi.org/10.15446/ing.investig.v38n3.73151.

Yacila, J., Camata, G., Salsavilca, J. and Tarque, N. (2019), "Pushover analysis of confined masonry walls using a 3D macro-modelling approach", *Eng. Struct.*, **201**, 109731. https://doi.org/10.1016/j.engstruct.2019.109731.

Yazdani, M. (2016), *Application of ANSYS Software in Civil Engineering*. Padideh Press (in Persian). https://doi.org/978-600-5464-74-0, 512.

Yazdani, M. (2021), "Three-dimensional nonlinear finite element analysis for load-carrying capacity prediction of a railway arch bridge", *Int. J. Civil Eng.*, **19**(7), 823-836. https://doi.org/10.1007/s40999-021-00608-w.

Yazdani, M. and Habibi, H. (2023), "Residual capacity evaluation of masonry arch bridges by extended finite element method", *Struct. Eng. Int.*, **33**(1), 183-194. https://doi.org/10.1080/10168664.2021.1944454.

Yazdani, M. and Zirakbash, M. (2024), "Assessment of masonry arch bridges retrofitted by sprayed concrete under in-plane cyclic loading", *Struct. Monit. Maint.*, **11**(1), 57-70. https://doi.org/10.12989/smm.2024.11.1.057.

Zhang, S., Yang, D., Sheng, Y., Garrity, S.W. and Xu, L. (2016), "Numerical modelling of FRP-reinforced masonry walls under in-plane seismic loading", *Constr. Build. Mater.*, **134**, 649-663. https://doi.org/10.1016/j.conbuildmat.2016.12.091.

JK